UDC 621.762.5:536.421.5

Tülay Yıldız*, Süleyman Aba
Fırat University, Faculty of Technology, Department of Metallurgical and Materials Engineering, Elazığ, Turkey
**tyildiz@firat.edu.tr*

The effect of sintering temperature on wear resistance of alloys produced by using hot isostatic pressing method

The present study investigated the effect of the temperature, at which a new matrix material was produced via hot isostatic pressing (HIP) method by adding certain rate of Co and Ni elements into CuSn (85/15) bronze alloy, and Co and Ni elements wear resistance of the samples produced. One of major advantages of HIP method is that heat and pressure are applied simultaneously during the sintering process. Thus, all or almost all of the pores are eliminated during the manufacturing and a denser material is obtained. During the study, sintering pressure and sintering time were kept constant as 15 min, and also sintering temperature was selected to be 700 and 800 °C as the variable parameter. Sintering process was carried out under vacuum starting from the first burn. The produced samples were then prepared metallographically and SEM and EDS analyses were performed for microstructure examinations. Microhardness of the samples was taken to investigate mechanical behaviors of the samples and they were subjected to wear test. Finally, density test was applied to samples and their experimental and theoretical densities were calculated. In conclusion, it was seen that more homogenous samples were obtained as sintering temperature increased. As Co amount and temperature increased in the study, wear resistance increased.

***Keywords**: hot ısostatic pressing, powder metallurgy, microhardness, abrasive wear.*

INTRODUCTION

New material technologies require the improvement of material characteristics such as wear and corrosion resistance and strength properties. Powder metallurgy (PM) has much to offer because sintering of powder materials produces materials of extremely fine and uniform microstructure and enables the formulation of materials composed from different constituents yielding unique property combinations [1–3].

The wear resistance of the composite was found to be much higher than that of the matrix alloy. It expands with expanding the molecule content as the hard particulates resist the wear action of abrasion and give protection to the surface, meaning that; when the content increases, the wear resistance will be enhanced [4].

Powder metallurgy is a general name given to the technique of shaping pure metal and alloy metal powders in a mold and bringing the strength to them with heat treatment (sintering). In recent years, the number and variety of parts produced by powder metallurgy method have increased. Main reasons for this are affordability, their high strength as well as low densities and production for specific uses [5]. Hot isostatic pressing (HIP), which is one of the production

methods of powder metallurgy, is a method containing high pressure gas in which pressure is applied isostatically to one or more parts in order to produce completely dense materials [6].

Co and Ni powders are used in an opposite amount to the Cu–Sn contribution as diamond-binding phase in accordance with their good wetting properties. Cu–Sn addition can be in the form of a mixture of Cu and Sn powders or in the form of pure bronze powder. The manufacturer specifies the use mode with the pressure sintering application characteristic [7]. The best result in bronze-based material production and abrasion tests performed after the production with the powder metallurgy method by adding ceramic powder in different types and rates was obtained at 350 MPa pressing pressure and at 820 °C temperature. It was found from the microstructure images that low-melting powders in the material formed liquid phase sintering and accordingly the pores shrank. It was also observed that some of the metal powders with low melting temperature evaporated during sintering [8].

Park et al. joined FeCrAl and Zr alloys with HIP method for melting energy applications. In the study, they chose the HIP temperatures between 700 °C and 1050 °C. They evaluated the mechanical properties of HIPped samples with four-point bending and tensile tests. They obtained higher strengths from the samples obtained with HIP at 700 °C. They stated that with increasing HIP temperature, the diffusion layer forming in the interface and its thickness increased and intermetallic compound and cavity were not observed at the interface up to 950 °C [9]. Tam et al., investigated the effects of temperature on production of Cr and Si by hot isostatic pressing. They examined the microstructures and porosity properties of the samples. As a result of the study, they determined the optimum temperature as 1373 K [10]. Elrakayby et al., investigated the condensation behavior of nickel alloy powder during the hot isostatic pressing by using the finite elements method [11]. Chang et al., examined the effect of temperature on microstructure and tensile properties by using hot isostatic pressing method in the compacting of Inconel 718 powder. They noted that the density of MC carbide particles decreased with increasing temperature and a yield resistance of 0.2 % formed with increasing HIP temperature [12]. Copper-based materials are generally used as plain bearing material owing to their properties such as high corrosion resistance, high thermal and electrical conductivity, self-lubrication, and high wear resistance [13]. Role of tin having an anti-friction property among copper-based materials is important for wearing. Copper-based tin bronzes containing tin are used as bearing material because they display high resistance to wear [14]. Friction and wear properties of these materials are proportionally positively influenced by the rate of tin in manufactured parts [15, 16]. Amount of bronze compound used in cases where intensive matrix wear is expected is increased by 70 % and the amount of bronze is decreased only to quantity of filling stage (< 5 %) that is required to cover pores when low wear is expected. Based on their well wetting property, powders of Co and Ni are used in a reverse proportion to Cu–Sn addition as diamond bonding stage. Cu–Sn addition can be in the form of a mixture of Cu and Sn powders or pure bronze powder. Producer determines the way of use by characteristic of pressure sintering [7]. In their study, Karagöz et al., changed the conditions of sintering by keeping constant the matrix compound, consisting of powder grains from Co, Ni and Cu + Sn. As a result of field studies and bending strength tests, the best result was obtained at 730 °C with sintering time of 15 min [17]. In their study, Boz and Kurt produced bronze-based brake pads by using powder metallurgy method and tested friction-wear performances of the produced brake

pads. At the second stage, they produced by adding Zn powder of 0.5–0.4 % into bronze-based pad powders and compared the two materials by applying the same tests. While the optimum wear resistance was identified in the sample containing 0.5 % Zn, the optimum friction coefficient was identified in the sample containing 2 % Zn [18]. In their study, Ünlü et al., determined wear and mechanical properties of copper-based CuSn10, Fe-based Fe–graphite, FeCu–graphite, and bronze–iron-based CuSnFe–graphite bearings produced by P/M method and compared them with each other. As a result of the experiments, it was revealed that cast bearings had higher mechanical properties than bearings produced via P/M method [19]. The optimum result was obtained at 350 MPa of pressing pressure and at 820 °C in the production of bronze-based material via powder metallurgy method by adding various types and rates of ceramic powder and in the wear test made following the production [8]. In the study by Lin D. et al. VN alloy/Co-based composite coatings modified by Ti were prepared on a mild steel using laser cladding. The effect of Ti addition on the microstructure and wear resistance of VN alloy/Co-based coatings was investigated using optical microscopy, X ray diffraction, scanning electron microscopy, energy dispersive spectroscopy, transmission electron microscopy, microhardness tester and wear tester [20]. In the study by R. Ahmed et al., HIP-consolidation of cobalt-based Stellite alloys offerred significant technological advantages for components operating in aggressive wear environments. The aim of this investigation was to ascertain the effect of re-HIPing on the HIPed alloy properties for Stellite alloys 4, 6 and 20. Structure-property relationships are discussed on the basis of microstructural and tribo-mechanical evaluations. Re-HIPing results in coarsening of carbides and solid solution strengthening of the matrix. The average indentation modulus improved, as did in the average hardness at micro- and nano-scales. Re-HIPing showed improvement in wear properties the extent of which was dependent on alloy composition [21]. By considering the literature studies, the changes caused by cobalt and nickel elements at different rates in the matrix structure were investigated and abrasive wear test was applied to determine wear behaviors of the samples produced in the present study.

MATERIAL AND METHODS

In this study, a new matrix material was produced by adding Co and Ni elements into 85/15 bronze alloy at certain rates. In the study, the metal powders used were obtained in the grain size specified in Table 1.

Table 1. Grain sizes of the metal powders

Powder	Bronze (85/15)	Cobalt	Nickel
Size, μm	70	35	5

Before the sintering process, the powders were prepared in groups at the rates indicated in Table 2 in a powder weighing device (Fig. 1, *a*) with sensitivity of 1/1000. The proportionally prepared sample compositions were stirred for 20 min in the mixing unit. In order for the powders to be processed at a certain size and shape before sintering, the polyethylene glycol binder of 1 % was added to the mixture In order to make the mixing process more homogeneous, iron beads and chains at different diameters were left in the mixing cap. The samples were then subjected to pre-pressing process in the dimensions of 10×20×40 mm in the cold pressing machine (see Fig. 1, *b*). The pre-pressed samples were taken into pre-prepared graphite molds and made ready for sintering. In order to make the sintering process better, graphite mold was lubricated with a lubricant.

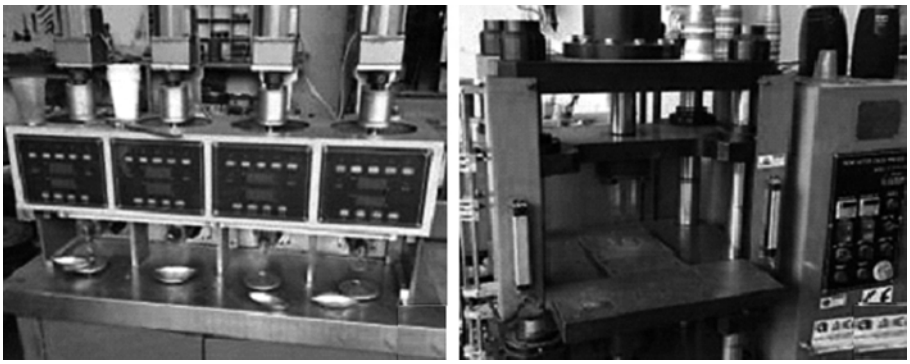

a *b*

Fig. 1. Powder weighing device (*a*), cold press (*b*).

Table 2. Weight distribution of sample groups

Group	Weight distribution of the sample groups, g				
	bronze (85/15)	cobalt	nickel	binder	total
S1–S2	205	0	6	4	215
S3–S4	193	12	6	4	215
S5–S6	180	25	6	4	215
S7–S8	168	37	6	4	215

The matrix samples were produced in Çel-mak industry and Commerce ltd. company. During the production of the samples, constant sintering pressure of 30 MPa, constant sintering time of 15 min and two sintering temperatures of 700 and 800 °C were used. While the sintering temperature is determined by taking 2/3 or 4/5 of the melting temperature of metal in single component systems, the sintering temperature in the systems with more than one component is selected below the melting temperature of the component with high melting temperature and above the melting temperature of the component with low melting temperature (Cu melting temperature was 1.085 °C and Sn melting temperature was 231.9 °C). The sintering temperature in the study was determined by considering the Cu–Sn dual balance diagram given in Fig. 2. The samples were produced with HIP

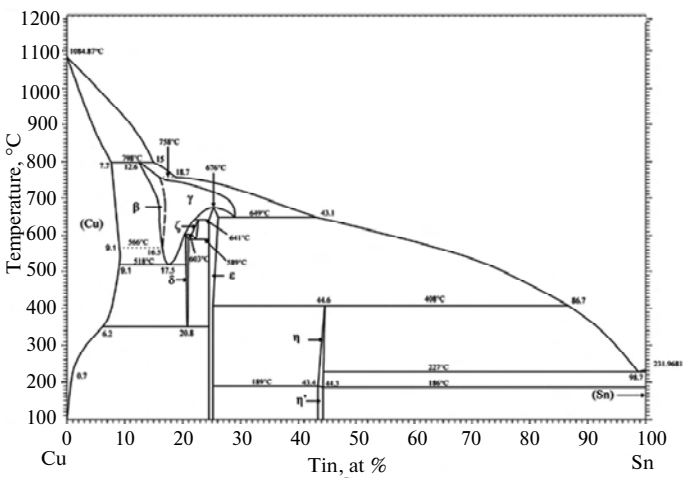

Fig. 2. Cu–Sn dual phase diagram [22].

method, a powder metallurgy production method. The sintering process was carried out under vacuum after the first burn. The samples were produced in dimensions of 10×10×40 mm (Fig. 3). Table 3 shows the amounts and the production parameters of the metal powders used during the production.

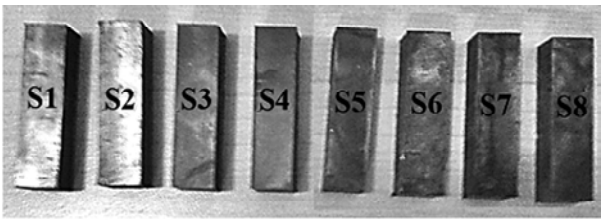

Fig. 3. Samples produced by the HIP method.

Table 3. Production parameters of the samples

Group	Sintering pressure, MPa	Sintering temperature, °C	Sintering time, min	Bronze, %	Cobalt, %	Nickel, %
S1	30	700	15	97	0	3
S2	30	800	15	97	0	3
S3	30	700	15	92	5	3
S4	30	800	15	92	5	3
S5	30	700	15	87	10	3
S6	30	800	15	87	10	3
S7	30	700	15	82	15	3
S8	30	800	15	82	15	3

For the metallographic analysis of the produced samples, the surfaces of the samples were cleaned with 200, 320, 500, 800, 1000 and 1200 mesh sandpaper, respectively, and then polished with 3 μm diamond paste. Polished samples were subjected to etching process with pre-prepared etchant and EDS analyses were carried out to investigate the matrix material and to determine the compound of the compositions in the produced samples.

Microhardness measurement was made under a load of 500 g, at waiting period of 10 s, and at a distance of 1 mm to determine hardness of the samples produced via HIP method. The samples were then subjected to abrasive wear test to determine wear resistance of the samples. Abrasive wear samples were worn once they were prepared in the sizes of 10×10×10 mm. Figure 4 shows abrasive wear apparatus and its parts. Abrasive wear test was performed by abrasion of surface of the sample. The tests were carried out using abrasion apparatus with pin-on disc system. Abrasive wear tests were applied using 120 mesh SiC sanding cylinder and applying two different loads, 5 and 15 N. Wear test was applied individually under every load at 10, 20, 30 m distances. In the abrasive wear tests carried out on turning lathe rotation speed and feed rate were chosen as 16 rpm and 2.8 mm, respectively. By taking the diameter of abrasive sanding cylinder into account, total distance was determined by calculating circumference of the cylinder. Operation of

turning lathe was based on 16 rpm. In the system, sample works by applying a load to abrasive from the top with a straight angle of 90°.

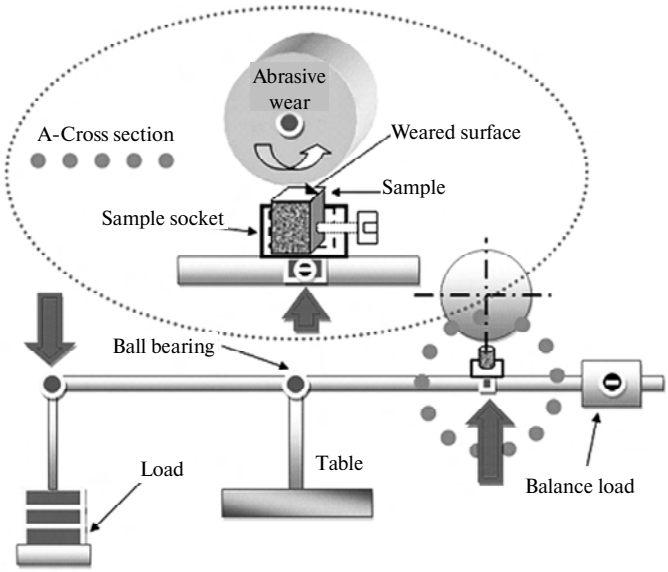

Fig. 4. Wearing device and parts [23].

DENSITY CALCULATION

The density measurements of the samples produced with the HIP method were calculated according to Archimedes' principle. The density measurements were performed with the AD-1653 brand density measurement kit in Fig. 5. Firstly, the weight of the samples in air and then their weight in water were measured and their experimental densities were determined with the help of the formula used for determining the density with the density measurement kit:

Fig. 5. Precision scale and density measurement kit [24].

$$\rho = \frac{W}{G} Rho \text{ , g/cm}^3, \qquad (1)$$

where ρ – density, g/cm^3; W – weight of the samples in air, g; G – weight of the samples in water, g; *Rho* – value taken from the catalog according to the water temperature, g/cm^3.

The theoretical densities of these samples whose experimental densities were determined were calculated with the help of the formula shown in equation

$$\text{Theoretical density} = (m_{\text{bronze}}\,\rho_{\text{bronze}}) + (m_{\text{Co}}\,\rho_{\text{Co}}) + (m_{\text{Ni}}\,\rho_{\text{Ni}}) + (m_{\text{binder}}\,\rho_{\text{polyethyleneglycol}}), \quad (2)$$

where m_{bronze}, m_{Co}, m_{Ni}, m_{binder} – the components' percentage by weight; ρ_{bronze} – 8.9 g/cm^3; ρ_{Co} = 8.9 g/cm^3; ρ_{Ni} = 8.9 g/cm^3; $\rho_{\text{polyethyleneglycol}}$ = 1.1239 g/cm^3.

RESULTS

Microstructure results

Figure 6 shows SEM images of S1 and S2 samples produced with no Co and 3 % nickel addition at 700 and 800 °C sintering temperature at 30 MPa sintering pressure and the EDS points taken from these samples. When these images were examined, it was observed that the grain boundaries became more apparent with increasing sintering temperature.

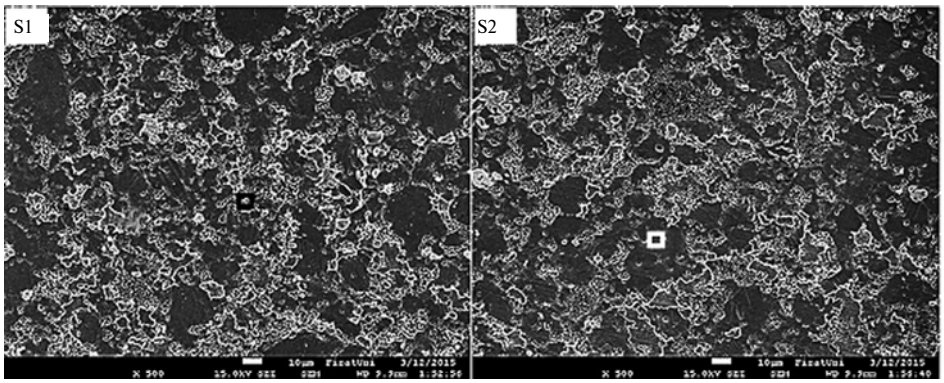

Fig. 6. SEM images of S1 and S2 samples.

Figure 7 shows SEM images of S3 and S4 samples produced with 5 % Co, 3 % nickel addition at 700 and 800 °C sintering temperatures at 30 MPa sintering pressure and the EDS points taken from these samples.

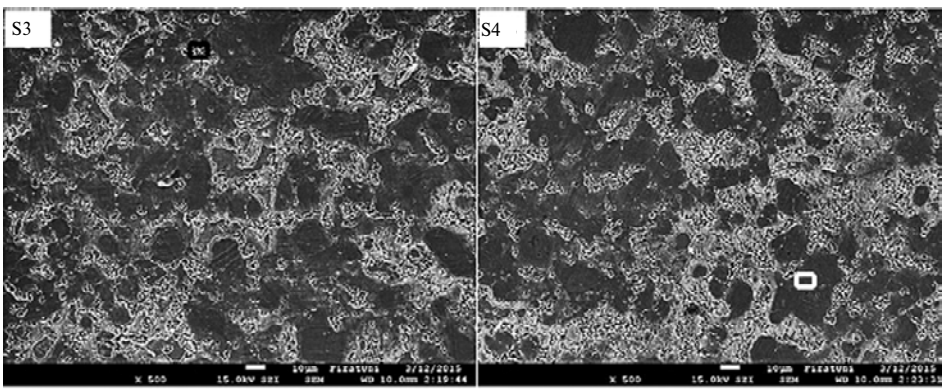

Fig. 7. SEM images of S3 and S4 samples.

Figure 8 shows SEM images of S5 and S6 samples produced with 10 % cobalt and 3 % nickel addition at 700 and 800 °C sintering temperatures at 30 MPa sintering pressure and the EDS points taken from these samples.

Figure 9 shows SEM images of S7 and S8 samples produced with 18 % cobalt and 3 % nickel addition at 700 and 800 °C sintering temperatures at 30 MPa

sintering pressure and the EDS points taken from these samples. It is seen that cobalt accumulated more in the grain boundaries in these samples and a more homogeneous distribution was observed with increasing temperature.

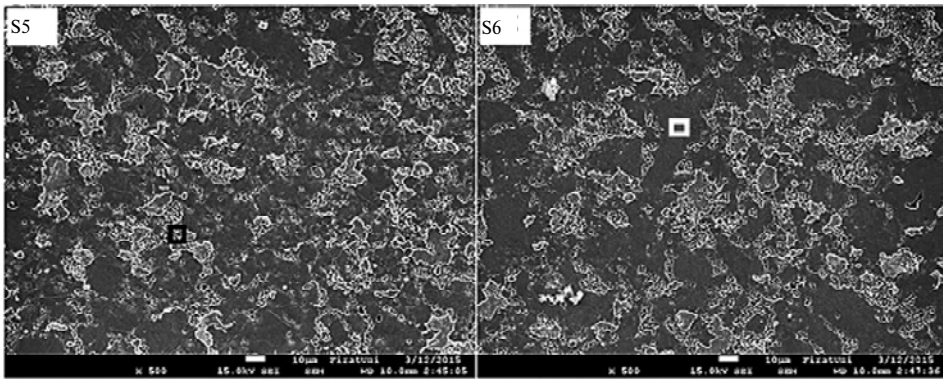

Fig. 8. SEM images of S5 and S6 samples.

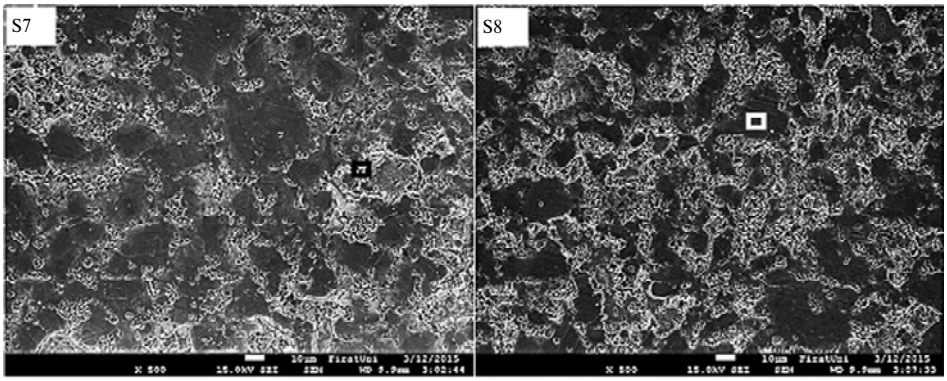

Fig. 9. SEM images of S7 and S8 samples.

In general, when the microstructure results were examined, all microstructure images obviously showed that since the sintering temperature was selected as 700 and 800 °C, the melting temperatures of Co element (1455 °C) and Ni element (1495 °C) could not be reached so these elements accumulated in grain boundaries without being dissolved. When the Cu–Sn balance diagram in Fig. 2 was examined, it was observed that the bronze liquefied at about 800 °C.

As is seen from Figs. 6–9, EDS analysis was applied to all of the samples without Co and with 5, 10, and 15 % Co addition from the marked points. Table 4 shows results of the analysis. When examining the table, it was seen that Ni element was dense at points where EDS was taken on the Co-free samples S1 and S2, the point, where EDS was measured, in the sample S3 with 5 % Co addition was the point where Co element condensed at 3.21 %, and Ni element condensed at 2.1 %. In the sample S4, EDS was measured from the point with 0.29 % Ni and 1.21 % Co element. EDS was measured from the point where Co element condensed (6.3 %) in the sample S5 and Ni element condensed (3.2 %) in the sample S6. Evaluation of EDS results of the samples S7 and S8 revealed that Co element (10.3 %) condensed without dissolving particularly in the grain boundaries in the sample S7. The point where EDS was measured was seen to contain 2.3 % Ni and 3.8 % Co element in the sample S8.

Table 4. EDS results

Sample No	Weight of element, %			
	Ni	Cu	Sn	Co
S1	3.1	82.7	12.7	–
S2	2.8	78.1	21.2	–
S3	2.1	81.2	14.8	3.21
S4	0.29	85.3	13.7	1.21
S5	2.3	73.1	15.3	6.3
S6	3.2	79.3	14.7	2.8
S7	2.8	72.3	14.8	10.3
S8	2.3	81.8	12.1	3.8

Microhardness results

Figure 10 shows microhardness graph of the samples S1, S3, S5 and S7 produced at 700 °C of sintering temperature. When examining this graph, it was observed that there was an increase in microhardness results as the rate of Co increased. While microhardness value of the sample S1 without Co addition produced at 700 °C of sintering temperature was 201 HV, it was 213 HV in the sample S7 with 15 % Co addition produced with sintering temperature of 700 °C.

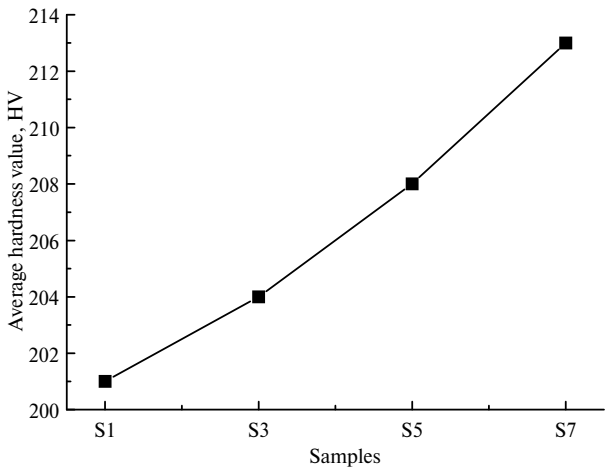

Fig. 10. Microhardness results of samples produced at 700 °C in different composition.

Figure 11 shows microhardness graph of the samples S2, S4, S6 and S8 produced at 800 °C of sintering temperature. When examining this graph, it was observed that there was an increase in microhardness values as the ratio of Co increased. While microhardness value of the sample S2 without Co produced at 800 °C of sintering temperature was 210 HV, it was 216 HV in the sample S8 with 15 % Co addition produced with sintering temperature of 800 °C.

Wear test results

Figure 12 and Table 5 show results of wear tests samples manufactured at 700 °C under 5 and 15 N loads.

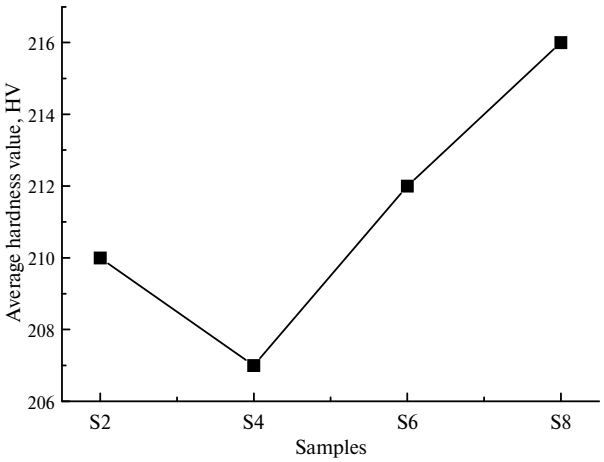

Fig. 11. Microhardness results of samples produced at 800 °C in different compositions.

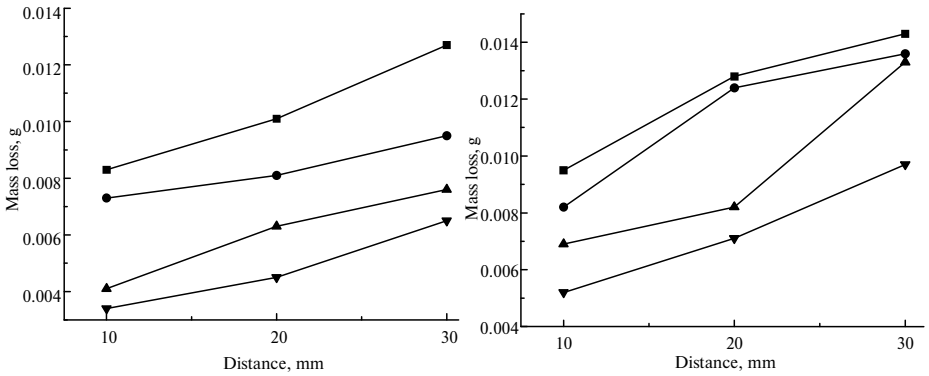

Fig. 12. Wear graphs of samples manufactured at 700 °C under 5 (*a*) and 15 (*b*) N loads: S1 (■), S3 (●), S5 (▲), S7 (▼).

Table 5. Wear results of samples produced at 700 °C

Group No	Load, N	Distance, m	Sintering pressure, MPa	Sintering temparature, °C	Bronz, %	Kobalt, %	Nikel, %	Difference, g
S1	5	10	30	700	97	0	3	0,0083
		20	30	700	97	0	3	0,0101
		30	30	700	97	0	3	0,0127
	15	10	30	700	97	0	3	0,0095
		20	30	700	97	0	3	0,0128
		30	30	700	97	0	3	0,0143
S3	5	10	30	700	92	5	3	0,0073
		20	30	700	92	5	3	0,0081
		30	30	700	92	5	3	0,0095
	15	10	30	700	92	5	3	0,0082
		20	30	700	92	5	3	0,0124
		30	30	700	92	5	3	0,0136

Table 5. (Contd)

S5	5	10	30	700	87	10	3	0,0041
		20	30	700	87	10	3	0,0063
		30	30	700	87	10	3	0,0076
	15	10	30	700	87	10	3	0,0069
		20	30	700	87	10	3	0,0082
		30	30	700	87	10	3	0,0133
S7	5	10	30	700	82	15	3	0,0034
		20	30	700	82	15	3	0.0045
		30	30	700	82	15	3	0,0065
	15	10	30	700	82	15	3	0,0052
		20	30	700	82	15	3	0,0071
		30	30	700	82	15	3	0,0097

Figure 13 and Table 6 show results of wear tests samples manufactured at 800 °C under 5 and 15 N loads. Wear tests was carried out with abrasive wear by using mass loss method under loads of 5 and 15 N at 10, 20, and 30 m distances. Results of wear tests were transferred into graphs by establishing the relationship between mass loss and distance loss. As is seen from the graphs, resistance to wear was generally determined to increase based on increased cobalt rate in all groups. Graphs of wear test results revealed that the samples S7 and S8 had the highest wear resistance. The lowest mass loss namely the highest wear resistance was determined in the sample S8 produced at 800 °C and under 30 MPa.

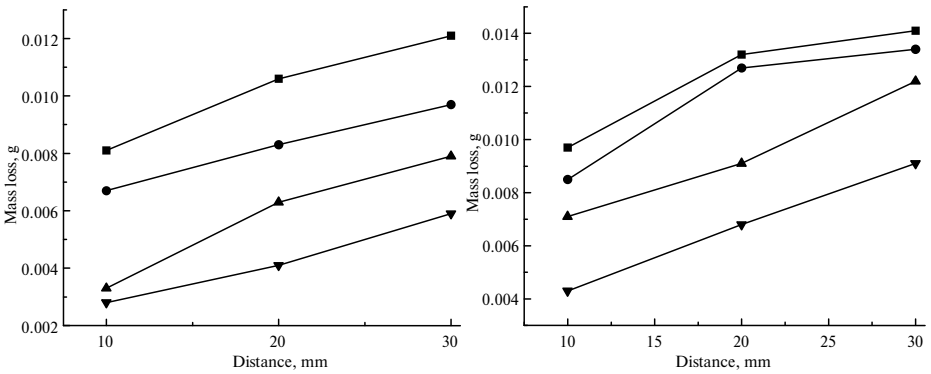

Fig. 13. Wear graphs of samples manufactured at 800 °C under 5 (*a*) and 15 (*b*) N loads: S2 (■), S4 (●), S6 (▲), S8 (▼).

Density measurement results

In order to get an idea about compressibility and condensation, density measurements of the samples produced by using HIP method were made. Table 7 shows the experimental and theoretical densities of the samples, whose weights are present in Table 2, produced at 30 MPa sintering pressure and with two different sintering temparature. Since densities of elements like Co (8.9 g/cm^3), Ni (8.9 g/cm^3) were not significantly different from each other, no significant difference occurred in the density values of the samples. It was found in the

literature that the closer the value of the experimental density to the theoretical density value, the less the amount of cavities in the samples [25].

Table 6. Wear results of samples produced at 800 °C

Group No	Load, N	Distance, m	Sintering pressure, MPa	Sintering temparature, °C	Bronz, %	Kobalt, %	Nikel, %	Difference, g
S2	5	10	30	800	97	0	3	0,0081
		20	30	800	97	0	3	0,0106
		30	30	800	97	0	3	0,0121
	15	10	30	800	97	0	3	0,0097
		20	30	800	97	0	3	0,0132
		30	30	800	97	0	3	0,0141
S4	5	10	30	800	92	5	3	0,0067
		20	30	800	92	5	3	0,0083
		30	30	800	92	5	3	0,0097
	15	10	30	800	92	5	3	0,0085
		20	30	800	92	5	3	0,0127
		30	30	800	92	5	3	0,0134
S6	5	10	30	800	87	10	3	0,0033
		20	30	800	87	10	3	0,0063
		30	30	800	87	10	3	0,0079
	15	10	30	800	87	10	3	0,0071
		20	30	800	87	10	3	0,0091
		30	30	800	87	10	3	0,0122
S8	5	10	30	800	82	15	3	0,0028
		20	30	800	82	15	3	0,0041
		30	30	800	82	15	3	0,0059
	15	10	30	800	82	15	3	0,0043
		20	30	800	82	15	3	0,0068
		30	30	800	82	15	3	0,0091

Table 7. Experimental and theoretical densities of the samples

Sample No	Sintering temperature, °C	Experimental density, g/cm^3	Theoretical density, g/cm^3
S1	700	8,798	8,878
S2	800	8,801	8,878
S3	700	8,881	8,931
S4	800	8,887	8,931
S5	700	8,891	8,911
S6	800	8,898	8,911
S7	700	8,701	8,747
S8	800	8,731	8,747

CONCLUSIONS

In this study, the production of a new matrix material was successfully carried out by using the constant sintering pressure, constant sintering time and different sintering temperatures by HIP method by adding Co into CuSn (85/15) bronze alloy at certain ratios.

The SEM images of the samples and the element distribution maps were examined. As a result of these investigations, it was observed that with the increase of sintering temperature, the grains accumulated and formed larger grains, and smooth and homogeneous structures formed. Additionally, it was observed Co was distributed on grain boundaries in Co added samples and they accumulated on grain boundaries as the amount increased.

When the microhardness results of the samples were evaluated, an increase was observed in the hardness values of all samples with both the increased sintering temperature and increased amount of Co.

When examining wear values of the samples, it was found that as amount of Co and sintering temperature increased, wear resistance increased.

When the theoretical and experimental densities of the samples were examined, it was seen that the difference was very small. Thus, it was concluded that the sample was produced in the minimum pore.

FUNDING

The research was supported by the Fırat University Scientific Research Projects Unit (Project No: TEKF.14.05)

Досліджено вплив температури, при якій новий матричний матеріал було отримано методом HIP (горячого ізостатичного пресування) при додаванні певного відсотка елементів Co і Ni до бронзового сплаву CuSn (85/15), а також елементів Co і Ni, на зносостійкість виготовлених зразків. Однією з головних переваг методу HIP є те, що нагрівання і тиск застосовуються одночасно у процесі спікання. Таким чином, всі або майже всі пори видаляються під час виготовлення і отримується більш щільний матеріал. При дослідженні тиск і час спікання були постійними протягом 15 хв, а також температуру спікання вибирали рівною 700 і 800 °C як змінний параметр. Процес спікання проводили під вакуумом, починаючи з першого відпалювання. Потім отримані зразки готували для металографічних досліджень, для мікроструктурних досліджень проводили SEM і EDS аналізи. Мікротвердість зразків вивчали для дослідження механічної поведінки, також випробували їх на знос. Було досліджено густину зразків, обчислено її експериментальні та теоретичні значення. Було виявлено, що більш гомогенні зразки отримано при збільшенні температури спікання, також при збільшенні кількості Co і значення температури підвищувалась їхня зносостійкість.

***Ключові слова**: HIP, горяче изостатичне пресування, порошкова металургія, мікротвердість, абразивний знос.*

Исследовано влияние температуры, при которой новый матричный материал был получен методом HIP (горячего изостатического прессования) путем добавления определенной доли элементов Co и Ni в бронзовый сплав CuSn (85/15), а также элементов Co и Ni, на износостойкость изготовленных образцов. Одним из основных преимуществ метода HIP является то, что нагревание и давление применяются одновременно во время процесса спекания. Таким образом, все или почти все поры удаляются во время изготовления, и получается более плотный материал. Во время исследования давление и время спекания поддерживали постоянными в течение 15 мин, а также температура спекания была выбрана равной 700 и 800 °C как переменный параметр. Процесс спекания проводили в вакууме, начиная с первого обжига. Полученные образцы затем были подготовлены для металлографических исследований, для микроструктурных исследований были выполнены SEM и EDS анализы. Микротвердость образцов изучали для исследования механического поведения

образцов, также их испытывали на износ. Исследовали плотность образцов, были рассчитаны ее экспериментальные и теоретические значения. Было виявлено, что более однородные образцы получены при повышении температуры спекания, также по мере увеличения количества Co и значения температуры повышается их износостойкость.

***Ключевые слова**: HIP, горячее изостатическое прессование, порошковая металлургия, микротвердость, абразивный износ.*

1. Kuhn H. Powder Metallurgy Processing. New York: Acad. Press., 1978.
2. Pokorska I. Experimental identification of yield stress for sintered materials. *Powder Metal. Met. Ceram*. 2008. Vol. 47, iss. 7–8. P. 393–397.
3. Pokorska I. Powder metallurgy materials in hot forming. *Powder Met.* 2007. Vol. 50, no. 4. P. 341–344.
4. Nassar A.E., Nassar E.E. Properties of aluminum matrix Nano composites prepared by powder metallurgy processing. *J. King Saud Univ. Eng. Sci.* 2017. Vol. 29. P. 295–299.
5. Yurtkuran E. T/M ile Üretilmiş Alüminyum Esaslı Malzemelerin Alaşım Elementleri ve Takviye Elamanı İçermelerine Bağlı Tel Erezyonda İşlenebilirliklerinin Araştırılması. Karabük Üniversitesi, 2011.
6. Conway J.J. and R.F.J. Hot isostatic pressing of metal powders. *Powder Metal Technol. Appl.* 2004. P. 49–53.
7. General E. Diamond Products for Sawing and Drilling Applications, GE Superabrasives, 1991.
8. Boz M. Seramik Takviyeli Bronz Esaslı Toz Metal Fren Balata Üretimi ve Sürtünme – Aşınma Özelliklerinin Araştırılması, Gazi Üniversitesi, Fen Bilim. Enstitüsü. Doktora Tezi. Ankara, 2003.
9. Park D.J., Kim H.G., Park J.Y., Il Jung Y., Park J.H., Koo Y.H. FeCrAl and Zr alloys joined using hot isostatic pressing for fusion energy applications. *Fusion Eng. Des.* 2016. Vol. 109–111. P. 561–564.
10. Tam C., Lee S., Chang S., Tang T., Ho H., Bor H. Effects of the temperature of hot isostatic pressing treatment on Cr–Si targets. *Cer. Int.* 2009. Vol. 35. P. 565–570.
11. Elrakayby H., Kim H., Hong S., Kim K. An investigation of densification behavior of nickel alloy powder during hot isostatic pressing. *Adv. Powder Technol.* 2015. Vol. 26. P. 1314–1318.
12. Chang L., Sun W., Cui Y., Yang R. Influences of hot-isostatic-pressing temperature on microstructure, tensile properties and tensile fracture mode of Inconel 718 powder compact. *Mater. Sci. Eng. A.* 2014. Vol. 599. P. 186–195.
13. Varol R., Sarıtas S. Investigation of the effect of ballistic fractures on the fatigue properties of iron based T/M parts. *First nation. Powder Met. Conf.* Ankara Gazi Univ., 1996. P. 407–418.
14. Prasad B.K. Dry sliding wear response of some bearing alloys as influenced by the nature of microconstituents and sliding conditions. *Metal. Mater. Trans. A.* 1997. Vol. 28. P. 809–815.
15. Backensto A.B. Effects of lubricants on the properties of copper-tin powders and compacts. *Advences P/M, Proc. PM Conf.* N. Jersey, 1990. P. 303–314.
16. Günther K.I.B. Self lubricating ıron base materials by mechanical alloying. *EURO PM 95 Proc.* 1995. P. 119–125.
17. Karagöz Ş., Zeren M. Wear characteristics of diamond cutting tools used in cutting marble. *Marble Turkey 3rd Symp. Report. Book.* Afyon, 2001. S. 452–461.
18. Boz M., Kurt A. The effect of zinc on friction-wear performance of powder metal brake pads materials. *Eng., Mim., Fak., Derg*. Gazi University, 2006.
19. Ünlü B.S., Yılmaz S., Varol R. Comparison of wear and mechanical properties of T/M bearing materials. *Makine Teknol. Electron. Bull*. 2005. Is. 2. P. 31–37.
20. Ding L., Hu S., Quan X., Shen J. Effect of aging treatment on microstructure and properties of VN alloy reinforced Co-based composite coatings by laser cladding, *Mater. Charact*. 2017. Vol. 129. P. 80–87.
21. Ahmed R., De Villiers Lovelock H.L., Davies S., Faisal N.H. Influence of Re-HIPing on the structure-property relationships of cobalt-based alloys, *Tribol. Int.* 2013. Vol. 57. P. 8–21.
22. Saunders N., Miodownik A.P. The Cu–Sn (copper–tin) system. *J. Phase Equilibria*. 1990. Vol. 11, no. 3. P. 278–287.

23. Gür A.K., Kaya S. Abrasive wear resistance optimization of three different carbide coatings by the Taguchi method. *Mater. Test.* 2017. Vol. 59, no. 5. P. 450–455.
24. Kati Yildiz N., Gür A.K. The effect of sintering temperature on microstructure and mechanical properties of alloys produced by using hot isostatic pressing method. *J. Alloys Compd*. 2018. Vol. 737. P. 8–13.
25. Topaloğlu F. The Characterization of Diamond Cutting Tips Used in Natural Stone Cutting of Cobalt Based Alloys as Bonding Matrix. Istanbul Technical Unıversity, 2013.

Received January 04.04.18
Revised January 02.07.18
Accepted April 03.07.18